Supporting Information

Chelator-Free Radiolabeling of SERRS Nanoparticles for Whole-Body PET and Intraoperative Raman Imaging

Matthew A. Wall[1,2†], Travis M. Shaffer[1,2†], Stefan Harmsen[1], Darjus-Felix Tschaharganeh[3], Chun-Hao Huang[3], Scott W. Lowe[3,4], Charles Michael Drain[2], and Moritz F. Kircher[1,5,6,7*]

1) Department of Radiology
Memorial Sloan Kettering Cancer Center
New York, NY, USA

2) Department of Chemistry
Hunter College and the Graduate Center, City University of New York
New York, NY, USA

3) Cancer Biology and Genetics Program
Memorial Sloan Kettering Cancer Center
New York, NY, USA

4) Howard Hughes Medical Institute
New York, NY, USA

5) Center for Molecular Imaging and Nanotechnology (CMINT)
Memorial Sloan Kettering Cancer Center
New York, NY, USA

6) Molecular Pharmacology Program, Sloan Kettering Institute
Memorial Sloan Kettering Cancer Center
New York, NY, USA

7) Department of Radiology
Weill Cornell Medical College of Cornell University
New York, NY, USA

†These authors contributed equally to this work.
*Corresponding author. E-mail: kircherm@mskcc.org

Contents

1. Supporting Tables

IR-780 gold nanoparticle pre-radiolabeled data			
Sample	**Z-average (nm)**	**PDI**	**Zeta potential (mV)**
SERRS NP at pH = 7.4	146.8, 145.7, 147.4	0.139, 0.128, 0.128	-35.5, -36.1, -35.1
Mean +/- standard deviation	146.6 +/- 0.9	0.132 +/- 0.006	-35.6 +/- 0.5

IR-780 gold nanoparticle post-radiolabeled data			
Sample	**Z-average (nm)**	**PDI**	**Zeta potential (mV)**
SERRS NP at pH = 7.4	131.5, 128.9, 131.6, 134.6, 130.6, 131.6	0.221, 0.225, 0.236, 0.231, 0.222, 0.242	-32.9, -33.6, -32.6, -34.5, -33.2, -33.9
Mean +/- standard deviation	131.5 +/- 1.9	0.230 +/- 0.006	-33.5 +/- 0.7

Table S1. Nanoparticle characterization before and after radiolabeling at pH = 7.4.

IR-780 gold nanoparticle pre-radiolabeled data			
Sample	**Z-average (nm)**	**PDI**	**Zeta potential (mV)**
SERRS NP at pH = 8.5	151.4, 148.5, 150.5	0.093, 0.110, 0.091	-46.8, -40.9, -41.0
Mean +/- standard deviation	150.1 +/- 1.5	0.098 +/- 0.010	-42.9 +/- 3.4

IR-780 gold nanoparticle post-radiolabeled data			
Sample	**Z-average (nm)**	**PDI**	**Zeta potential (mV)**
SERRS NP at pH = 8.5	123.8, 126.5, 124.9, 137.3, 141.4, 138.7	0.248, 0.216, 0.209, 0.231, 0.261, 0.244	-34.6, -33.8, -32.4, -30.3, -29.8, -29.1
Mean +/- standard deviation	132.1 +/- 7.9	0.235 +/- 0.020	-31.7 +/- 2.3

Table S2. Nanoparticle characterization before and after radiolabeling at pH = 8.5.

2. Supporting Figures

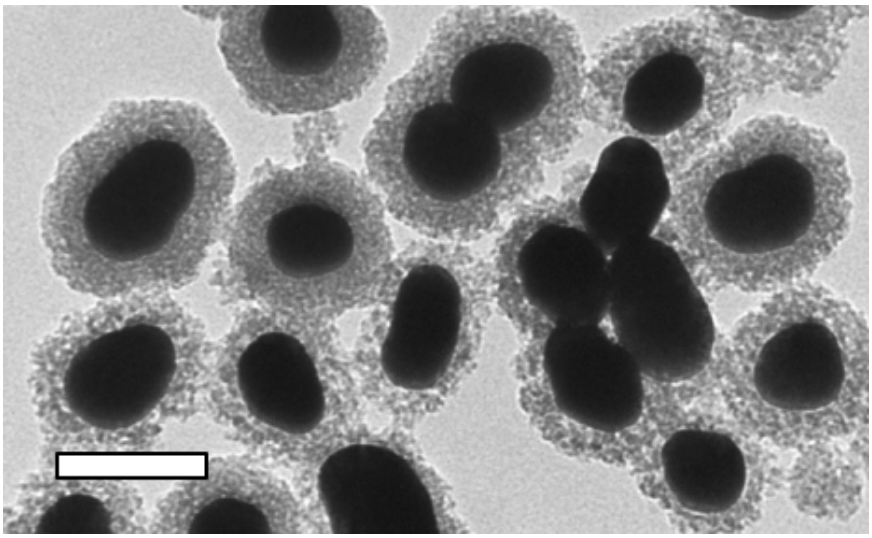

Figure S1. Degradation of silica shells after non-optimized radiolabeling with ^{68}Ga from KOH elution. TEM reveals that the silica shells become extremely porous and unstable after the ^{68}Ga radiolabeling procedure that had been optimized for pure silica nanoparticles. These nanoparticles rapidly degrade in serum. Scale bar is 100 nm.

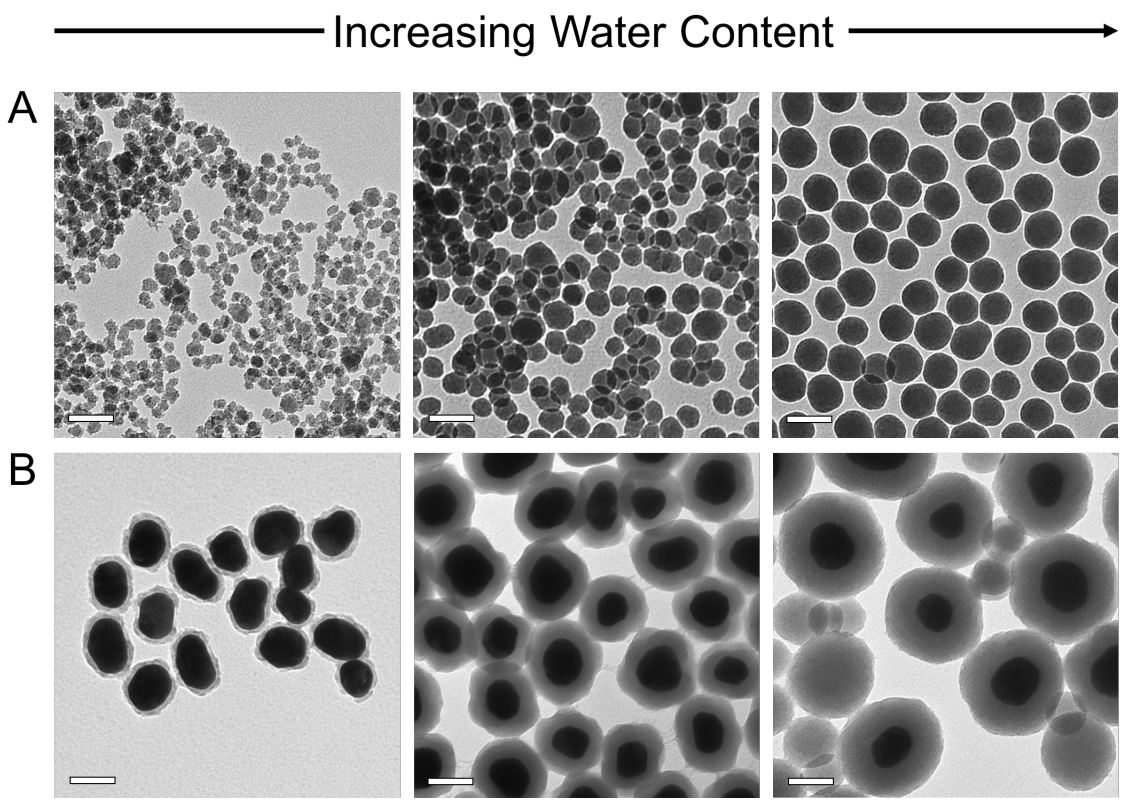

Figure S2. Influence of water content on silica nucleation and growth. (**A**) Synthesis of silica in the absence of gold nanoparticles. Silica was synthesized by a Stöber method in ethanol using (from left to right) 1.5 M, 3.0 M, and 4.5 M water for 1 h at room temperature. (**B**) Synthesis of silica in the presence of gold nanoparticles. Even though the water content is sufficiently high to homogeneously nucleate silica (from left to right, 3.25 M, 5.0 M, 7.5 M), the catalytic effect of the gold nanoparticle surface with respect to the condensation and aggregation of silica nuclei favors shell formation over silica nanoparticle growth. The syntheses in (B) only proceed for 25 min, compared to 1 h in (A). As the water content is increased beyond 5.0 M, free silica nanoparticles grow within 25 min. Alternatively, if the 3.25 M or 5.0 M syntheses were allowed to progress for 1 h a substantial amount of free silica nanoparticles would form. Scale bars are 100 nm in (A) and 50 nm in (B).

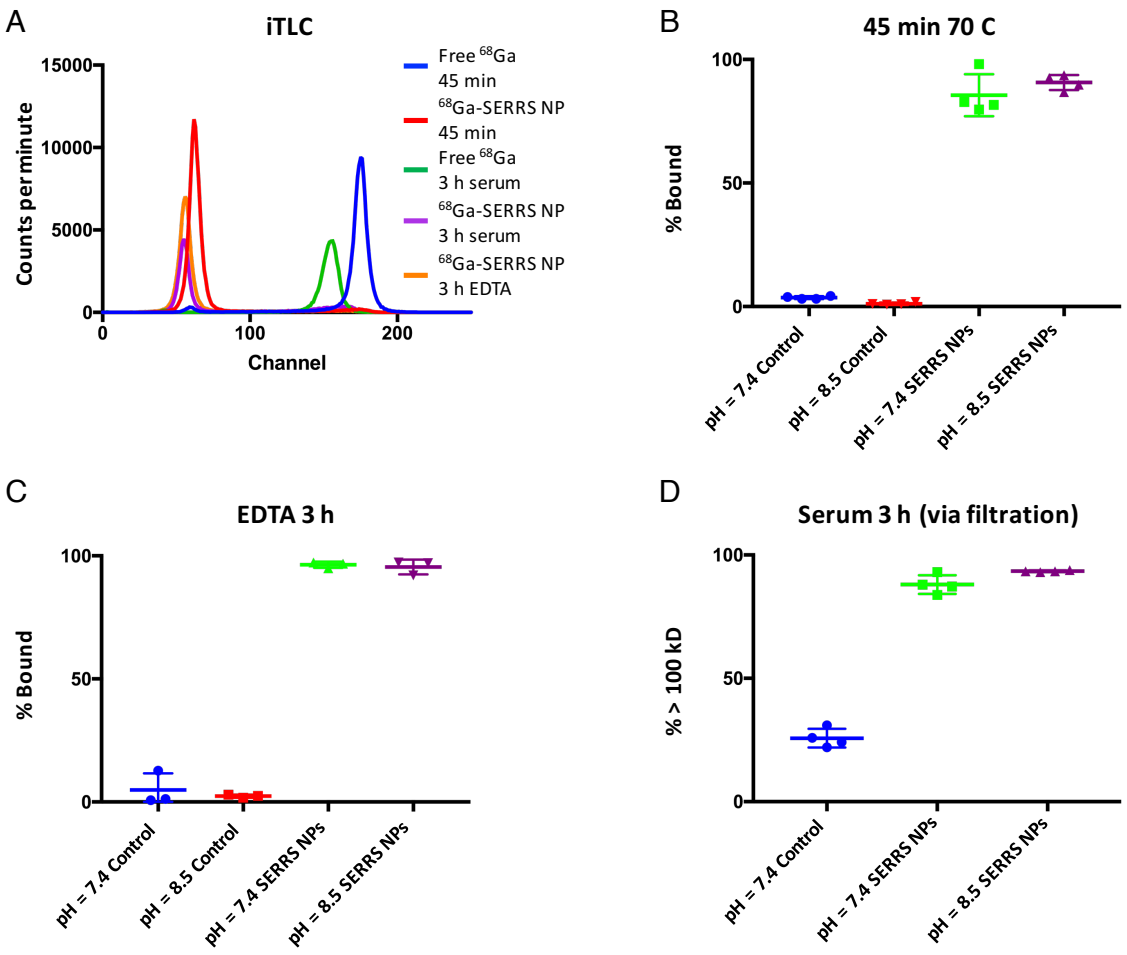

Figure S3. Radiolabeling characterization at 70 °C. SERRS nanoparticles were incubated with ^{68}Ga for 45 minutes at 70 °C then subject to characterization by iTLC and radioactivity measurements after separation with a 100 kD filter. (**A**) iTLC results show that ^{68}Ga stays at the origin after incubation with SERRS nanoparticles, but travels with the solvent front in the absence of SERRS nanoparticles. (**B**) The percentage of radioactivity bound to the nanoparticles after 45 minutes at 70 °C is estimated by the percentage of signal (integrated counts per minute) at the origin of the iTLC paper. (**C**) After radiolabeling at 70 °C for 45 minutes, the SERRS nanoparticles are exposed to EDTA which scavenges any loose ^{68}Ga. The percentage of radioactivity bound to the nanoparticles after EDTA challenge is estimated by the percentage of signal at the origin of the iTLC paper. Controls were conducted with EDTA added but without nanoparticles present. (**D**) The percentage of ^{68}Ga that remains bound to SERRS nanoparticles after exposure to 50% FBS at 37 °C for 3 h is estimated by separating the sample with a 100 kD filter and calculating the percentage of radioactivity contained in the > 100 kD fraction.

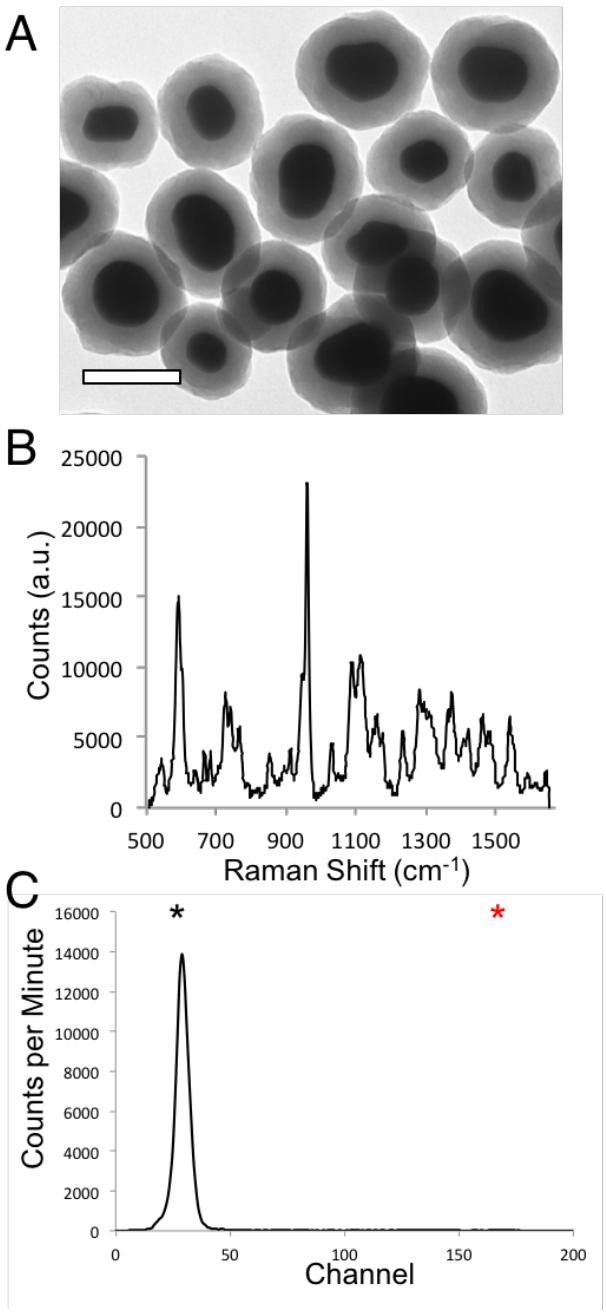

Figure S4. Characterization of room temperature radiolabeled PET-SERRS nanoprobes. (**A**) Transmission electron microscopy of PET-SERRS nanoparticles after radiolabeling at 25 °C for 5 minutes. (**B**) SERRS spectrum of the PET-SERRS nanoparticles in (A). (**C**) Instant thin layer chromatogram of PET-SERRS nanoparticles 5 minutes after addition of ^{68}Ga at room temperature. The black asterisk represents the origin of the iTLC paper (where the SERRS nanoparticles remain) and the red asterisk denotes the solvent front (where free ^{68}Ga would appear). However, the radiolabeled particles were not sufficiently stable in EDTA challenge or serum stability experiments (data not shown).

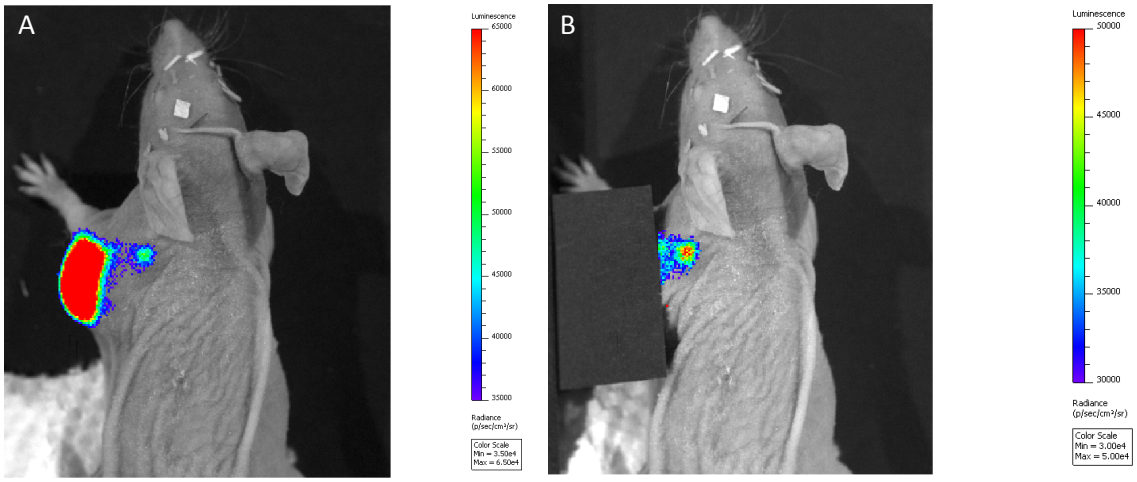

Figure S5. Cerenkov imaging of the LN with PET-SERRS NPs. (**A**) Entire area imaged. (**B**) Injection site covered.

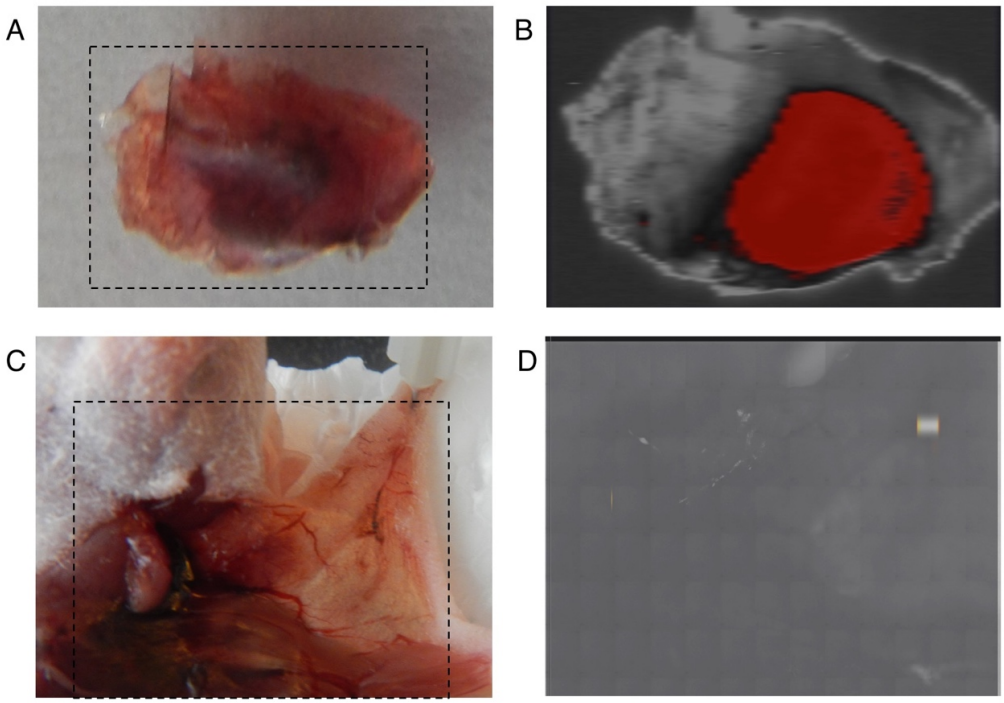

Figure S6. SERRS map of excised LN and resection bed. (**A**) Photograph of the same excised tissue shown in **Fig. 3C** of the main text. (**B**) SERRS imaging reveals that the LN (red) is completely contained within the resected specimen. (**C-D**) Photograph (C) and SERRS map (D) of the same resection bed shown in **Fig. 3C** of the main text shows that no SERRS contrast remained after resection, indicating clean surgical margins.

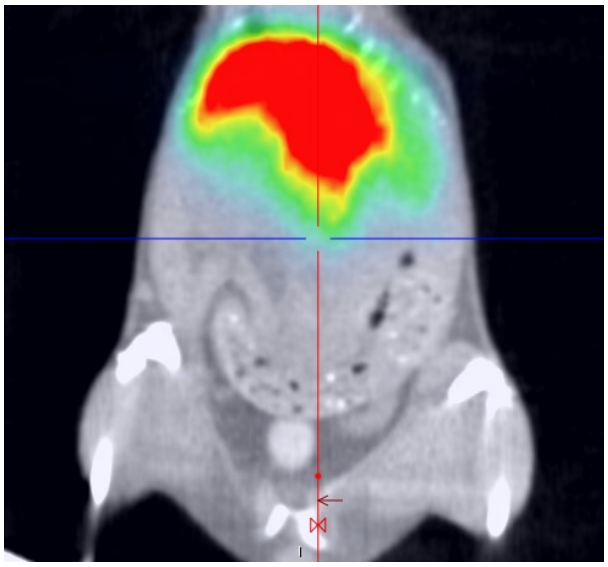

Figure S7. PET-CT image of wild type mouse 5 minutes after injection with PET-SERRS NPs, showing high activity in the liver.

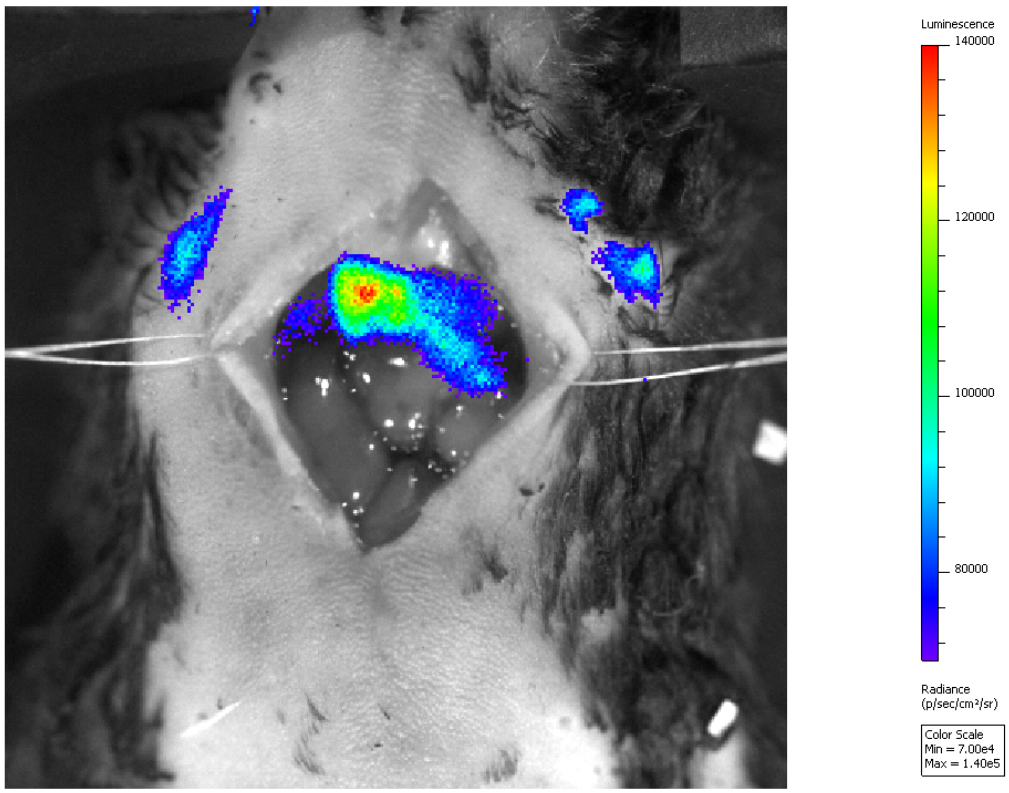

Figure S8. Cerenkov imaging of PET-SERRS NPs in healthy RES but not in cancerous tissue.

3. Experimental Section

Radiochemical yield: 1 μL samples were taken for radioactive instant thin layer chromatography (iTLC) at various time points over the course of 1 hour using silica-gel impregnated iTLC paper (Varian), and analyzed with a Bioscan AR-2000 radio-TLC plate reader. 0.1 M citric acid (pH = 4.2) was used as the elution solvent. The solution was centrifuged at 10000 rcf for 5 minutes, the supernatant removed and counted, and the product re-dispersed in 10 mM MES buffer in order to achieve purification.

The centrifugal pelleting approach to determining radiochemical yield proceeded by centrifugation of radiolabeled nanoparticles at 10000 rcf to create a pellet at the bottom of the Eppendorf tube, removal of supernatant, re-dispersion of the pellet in 10 mM MES and measurement of its radioactivity. Control solutions, absent of nanoparticles, were conducted for both iTLC and pelleting to determine any gallium precipitate formation.

Serum Stability Studies: Serum stability experiments were performed at 37 °C in a mixture of 50% fetal bovine serum (FBS, Gemini Bio-products) and 50% buffer (total volume 150 μL) on an Eppendorf thermomixer at 550 rpm. Both iTLC and size exclusion filtration analysis (100 kD filters) were completed. The size exclusion filtration analysis was conducted by placing 10 μL of 50 mM EDTA (pH 7) into the serum samples for 10 minutes, after which the samples were placed in the size exclusion filter and spun down at 10000 rcf for 5 minutes. Samples were washed twice, and the activity in the filter was measured and compared to the radioactivity that passes through the filter. Controls were ran absent of nanoparticles. The value reported in the main text is that measured by iTLC, which showed more free activity and was therefore considered to be a lower-bound estimate.

EDTA challenge Studies: After purification, 10 μL of 50 mM EDTA (pH 7) was added to each sample and incubated at RT for 3 hours. Samples were then ran on iTLC as described in the radiochemical yield section. Controls were ran absent of nanoparticles.